International Journal of Fluid Power 7 (2006) No. 3 pp. 29-39

A REVIEW ANALYSIS OF UNSTEADY FORCES IN HYDRAULIC VALVES

Giuseppe Del Vescovo[1] and Antonio Lippolis[2]

[1] *Dipartimento di Ingegneria Meccanica e Gestionale, POLITECNICO di BARI - Via Re David 200 - 70125 Bari - Italy*
g.delvescovo@poliba.it,
[2] *Dipartimento di Ingegneria dell'Ambiente e per lo Sviluppo Sostenibile , POLITECNICO di BARI - V.le del Turismo, 8 74100 Taranto - Italy*
lippolis@poliba.it

Abstract

In the fluid power applications where the typical operating conditions are dynamic the knowledge of the unsteady flow forces that act on the spools of the hydraulic valves represents an important issue to be addressed in order to make a correct design of the valve geometry and its driving system.

This paper deals with a rigorous unsteady numerical study of the fluid dynamic behavior of a hydraulic directional control valve.

A theoretical approach based upon the application of the momentum equation in the transient fluid dynamic conditions is presented, while a successive numerical analysis is performed by using the commercial Fluent™ code that provided, in the past, a correct evaluation of the stationary flow forces.

Unsteady simulations have been carried out considering three different conditions: constant pressure boundary conditions during the spool movement, inlet pressure ripple at a constant spool position, damped pressure oscillations during the spool opening phase.

The main objective is to estimate the critical magnitude orders of the pressure ripple frequency and of the axial spool velocity above which the pseudo-steadiness assumption fails; in order to reach this aim, in some cases, the effects of the fluid dynamic phenomena connected with the unsteady flow conditions have been amplified.

Keywords: CFD simulation, unsteady flows, directional control valves

1 Introduction

Commercial CFD (Computational Fluid Dynamics) codes are considered by fluid power researchers as new powerful tools to optimize the design of the hydraulic components and to study their fluid dynamic performance.

Before the spreading of these numerical methods a theoretical approach (Merrit, 1967) has been traditionally used in order to provide simple analytical relations useful to predict the fluid dynamic behaviour of the hydraulic valves.

By using CFD codes more design and optimization iterations can be made by using computer simulations replacing expensive experimental campaigns. Nowadays, these techniques do not require necessarily deep competencies in the Computational Fluid Dynamics, thus leaving to the engineers the task to critically analyze the solution by testing its physical validity. The numerical techniques have provided in the past very important indications about the compensation technique (Borghi et al, 2000), the optimization of the notch geometry (Macor et al, 1999, 2000, 2002) the effects of wall shear forces (Yang, 2006), the three dimensional effects of the valve geometry and the analysis of open center and proportional directional control valves (Del Vescovo et al, 2002, 2003, 2004); all these simulations refer only to steady state conditions.

As far as the unsteady analysis is concerned, the traditional approach starts from the quasi-static assumption of the efflux conditions. In this way some remarkable simplifications are possible because this approach does not require unsteady numerical simulations. In fact, the flow force can be treated as the sum of two terms (Borghi et al, 1998, Nervegna 2000, Krishnaswamy et al, 2002): the first is the steady component, the latter is the so-called unsteady component and is directly connected to the effects of the fluid inertial properties. The unsteady component can be evaluated by using the flow rate values computed by means

This manuscript was received on 14 October 2005 and was accepted after revision for publication on 27 September 2006

of steady state simulations.

The separated study of these two components has allowed researchers to modify the dynamic performance of a servovalve (Krishnaswamy et al, 2002) manipulating a geometric length called in literature "*damping length*".

The aim of this paper is to provide a rigorous numerical unsteady analysis avoiding the simplification deriving from the quasi-static assumption.

The "*dynamic mesh*" technique, used in this work, allows the movement of the boundary regions inside the valve while the computational mesh is updated at every time step. This technique has been successfully used in literature (Huguet, 2004) to simulate the fluid dynamic field in a direct relief valve during the plug movement.

The User Defined Functions (UDF's) have been used in the code in order to update the pressure boundary conditions.

This paper aims to provide indications about the pressure ripple frequency and the spool velocity values above which the pseudo-steadiness hypothesis fails.

2 Theoretical Approach

In this section a theoretical approach will be used in order to identify the most important topics of the discussion that will be faced by the unsteady CFD analysis. For clarity of exposure, a spool directional control valve will be taken as reference but the analysis, and the derived conclusions, is easily extendible to other hydraulic components.

With reference to the control volume presented in Fig. 1 the momentum equation can be applied in its integral form:

$$\frac{d}{dt}\iiint_{CV}\rho\vec{v}dV = -\oiint_{S}(\rho\vec{v}\cdot\vec{n})\vec{v}dS+\oiint_{S}\bar{\sigma}dS+\iiint_{CV}\rho\vec{f}dV \tag{1}$$

where ρ is the fluid density, $\bar{\sigma}$ is the stress vector, $\bar{f}$ represents the body forces per unit mass, $\bar{v}$ is the fluid velocity.

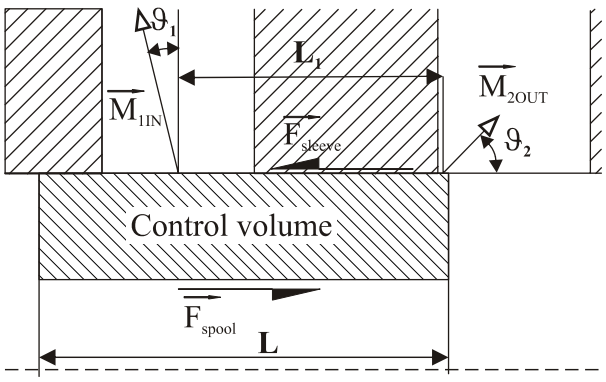

Fig. 1: *Control volume*

Considering the axial component of Eq. 1, the following scalar equation can be derived:

$$\frac{d}{dt}\iiint_{CV}\rho v_{ax}dV = -\oiint_{S}(\rho\vec{v}\cdot\vec{n})v_{ax}dS+\oiint_{S}\vec{\sigma}\cdot\vec{i}dS \tag{2}$$

The second integral of the right hand side of Eq. 2 represents the sum of all the viscous and pressure forces acting axially on the control volume.

From the integration the following formula can be deduced:

$$\oiint_{S}\vec{\sigma}\cdot\vec{i}dS = F_{spool}-F_{sleeve} \tag{3}$$

where F_{spool} represents the spool force that acts on the fluid (equal and opposite to the flow force) and F_{sleeve} represents the body valve viscous force that acts on the control surface.

The first term of the RHS of Eq. 2 can be easily written in the form:

$$\oiint_{S}(\rho\vec{v}\cdot\vec{n})v_{ax}dS = M_{1ax}-M_{2ax} \tag{4}$$

where M_{1ax} and M_{2ax} are the axial components of the momentum flows entering and exiting the control volume.

Finally the following equation can be deduced:

$$F_{spool} = F_{sleeve}+M_{2ax}-M_{1ax}+\frac{d}{dt}\iiint_{CV}\rho v_{ax}dV \tag{5}$$

In the previous expression the unsteady term is clearly notable and will be later detailed. However, it must be underlined that the other terms are influenced by the unsteady flow conditions as well. For example, the influence of the boundary layer on the velocity profile in the metering section in unsteady conditions is different from the influence exerted in steady conditions; this phenomenon influences the flow rate value and affects, implicitly, the values of the momentum flows M_{1ax} and M_{2ax}.

If the unsteadiness of the efflux conditions are of secondary importance, the difference between steady and unsteady flow force values relies almost completely in the time derivative term of Eq. 5 that is strictly connected to the fluid inertial properties. This paper tries to identify the fluid dynamic cases where this hypothesis can be considered valid.

With the hypothesis that the fluid density does not change with the position in the control volume, the unsteady term can be expressed as follows:

$$\frac{d}{dt}\iiint_{CV}\rho v_{ax}dV = \iiint_{CV}\frac{d}{dt}\rho(v_{rel}+v_{spool})dV = \tag{6}$$

$$\begin{aligned}
&= \frac{d\rho}{dt}\iiint_{CV}(v_{rel}+v_{spool})dV + \\
&+\rho\iiint_{CV}(a_{rel}+a_{spool})dV = \\
&= \frac{d\rho}{dt}\iint_{A}v_{rel}dA\int_{0}^{L}dx+\frac{d\rho}{dt}v_{spool}\ V_{CV}+ \\
&+\rho\iint_{A}a_{rel}dA\int_{0}^{L}dx+\rho\ a_{spool}V_{CV} = \\
&\frac{d\rho}{dt}\iint_{A}L_{axial}dq+\frac{d\rho}{dt}v_{spool}\ V_{CV}+ \\
&+\rho\frac{d}{dt}\iint_{A}L_{axial}dq+\rho\ a_{spool}V_{CV} =
\end{aligned} \tag{7}$$

Assuming a reference system moving with the spool, the absolute velocity v (and acceleration a) has been expressed as the sum of the instantaneous spool velocity v_{spool} (acceleration a_{spool}) and the velocity $v_{rel,}$ (acceleration a_{rel}) relative to the spool.

L_{axial} indicates the axial extension of each elementary stream tube characterized by the flow rate dq,

By using the mean value theorem for integrals the following equation can be written:

$$\iint_A L_{axial} dq = QL_1 \tag{8}$$

where L_1 is the mean axial length of the elementary stream tubes; reasonably, L_1 is equal to the distance between the middle point of the Inlet port and the middle point of the metering section (see Fig. 1).

Assuming that L_1 is independent on the time, the time derivative of the integral can be written as follows:

$$\frac{d}{dt}\iint_A L_{axial} dq = \dot{Q}L_1 \tag{9}$$

It is obvious that the length L_1 is not constant but in the case of spool opening it increases with the simulation time. This approximation is strong if the ratio of the axial spool opening to the length of the control volume is not negligible but the aim of this theoretical approach is to provide a flow force unsteady term that can be easily computed. This term will be compared to the difference between steady and unsteady flow forces computed by the numerical simulations giving rise to important observations about the importance of the inertial forces.

In this way, the following simplified relation can be derived for the unsteady term of Eq. 5:

$$\frac{d\rho}{dt}QL_1 + \frac{d\rho}{dt}v_{spool}V_{CV} + \rho\dot{Q}L_1 + \rho a_{spool}V_{CV} \tag{10}$$

The two components of Eq. 10 connected with the compressibility of the oil are negligible. This is due to the very low oil compressibility. To better underline this observation a non-dimensional coefficient can be defined as the ratio of the first to the third term of the Eq. 10:

$$\Pi_C = \frac{\frac{d\rho}{dt}QL_1}{\rho\ \dot{Q}L_1} = \frac{dp}{dt}\frac{Q}{\beta\dot{Q}} = \frac{dp}{dt}\frac{\sqrt{\Delta p}}{\beta\frac{1}{2}\frac{dp}{dt}\frac{1}{\sqrt{\Delta p}}} = \frac{2\Delta p}{\beta} \tag{11}$$

where the oil compressibility equation and the orifice equation have been implicitly used.

Considering the typical pressure drops in a hydraulic plant and the bulk modulus value, the last ratio can reach, in the extreme cases, 5 % and usually much lower values.

The second term of Eq. 10 connected with the spool velocity is negligible; this statement can be shown by introducing the following non-dimensional coefficient as the ratio of the second term to the first one:

$$\Pi_v = \frac{\frac{d\rho}{dt}v_{spool}V_{VC}}{\frac{d\rho}{dt}QL_1} = \frac{v_{spool}}{v_r}\left(\frac{A}{A_r}\right)\left(\frac{L}{L_1}\right) \tag{12}$$

where A_r is the restricted section area and v_r is the normal velocity in the restricted section.

Considering the typical magnitude order of the spool velocity in commercial valves (~0.1 m/s) and of the flow velocity in the restricted section (~100 m/s), it can be concluded that the Π_v value is very low (the other factors being of magnitude order from 1 up to 10 except for the very small openings).

The last observation confirms that the second term is negligible if compared to the first one, and consequently it is negligible if compared to the term $\rho L_1\dot{Q}$.

Finally, the ratio of the forth term to the third one can be analyzed:

$$\Pi_i = \frac{\rho a_{spool}V_{VC}}{\rho\dot{Q}L_1} = \frac{a_{spool}AL}{\dot{Q}L_1} \tag{13}$$

Assuming as uniform the acceleration of the spool, the following formula can be derived:

$$a = \frac{2\ \Delta s}{\Delta t^2} \tag{14}$$

Considering the magnitude orders of the displacement (~1 mm), and of the spool opening time (~10 ms) the acceleration equals 10 m/s^2.

The ratio of the maximum flow rate to the spool opening time gives an average value of flow rate time derivative:

$$\dot{Q} = \frac{C_d A_{rmax}\sqrt{\frac{2\Delta p}{\rho}}}{\Delta t} \tag{15}$$

where A_{rmax} is the maximum value of the restricted section surface area.

Consequently:

$$\Pi_i = \frac{a_{spool}}{\frac{C_d\sqrt{\frac{2\Delta p}{\rho}}}{\Delta t}}\left(\frac{A}{A_{rmax}}\right)\left(\frac{L}{L_1}\right) \tag{16}$$

The magnitude order of the first denominator term is 10^{-3} while the other factors are of magnitude order 1 so indicating that this parameter can be reasonably neglected.

Finally the flow force is given by the equation:

$$F_{spool} = F_{sleeve} + M_{2ax} - M_{1ax} + \rho L_1\dot{Q} \tag{17}$$

where only one component of the time derivative term should be considered.

In conclusion, a complete unsteady analysis highlights two different problems: the analysis of the so-called "unsteady flow force component" that has been reduced to only one predominant term and the study of the difference between steady and unsteady efflux conditions that affects implicitly the terms M_{1ax} and M_{2ax} of the Eq. 17.

3 Description of the Geometry and of the Computational Grid

The unsteady numerical simulations have been realized by using the "*dynamic mesh*" technique.

This technique allows an unstructured computational mesh to be updated each time step. It is constituted by three different phases: "*relayering*", "*smoothing*", and "*remeshing*". The first phase adds or removes layers of cells adjacent to moving boundaries to keep the cell dimension at a specified value, the second phase realizes a repositioning of the nodes, the third phase prevents the presence of highly distorted cells that could lead to convergence problems. Different parameters can be specified before the iterations start in order to optimize the process; they have not been reported for the sake of brevity but they are detailed in the Fluent™ Manuals (Fluent Inc, 1995, 2000).

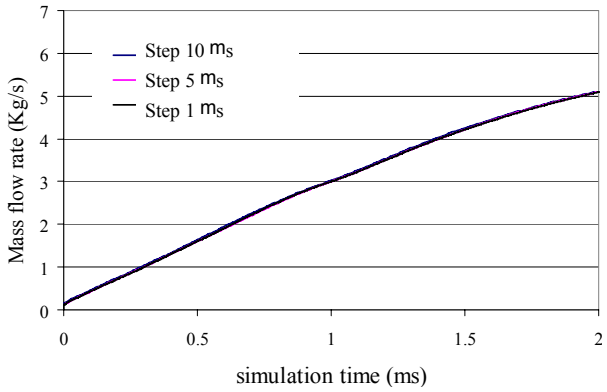

Fig. 2: *The discharged mass flow rate at three different integration time steps*

A preliminary phase to test the physical validity of numerical results has been realized. In particular three unsteady cases have been set with the same pressure drop and spool velocity values but with different integration time steps.

Figure 2 shows the results relative to three integration time steps (10 µs, 5 µs, 1 µs) and 2 ms spool opening time. The comparison of the three trends proves the physical validity of the numerical results and the reliability of the computational grid.

Figure 3 shows the images of the computational grids and the obtained velocity contours at two different axial spool displacements.

It can be noticed that a block structured grid has been used in the high pressure chamber while in the other regions an unstructured grid has been set because it is more suitable to the application of the "*dynamic mesh*" technique.

The zoomed images of the metering sections have been reported in order to better show the "*dynamic mesh"* process in the most critical region of the computational domain.

4 Numerical Results

The diagrams of Fig. 4 and Fig. 5 show the flow rate profiles at 30 bar pressure drop value and two different spool opening times, i.e. 20 ms and 2 ms. It must be considered that the first case coincides with the opening conditions of a commercial directional valve (spool velocity around 0.1 m/s) while the latter refers to prototype switching valves (spool velocity 1 m/s) and has been set to emphasize some fluid dynamic phenomena that will be later analyzed.

Moreover, the spool dynamics have been neglected because a uniform velocity has been set, while it is obvious that the spool movement has an initial acceleration phase and a final deceleration phase. The diagrams of Fig. 4 and Fig. 5 show that, in the case of 20 ms spool opening time, the discharged mass flow rate profile in unsteady conditions is almost overlapped to the profile obtained in steady conditions.

A slight difference is noticed if the spool velocity is one magnitude order greater than the previous case (Fig. 5).

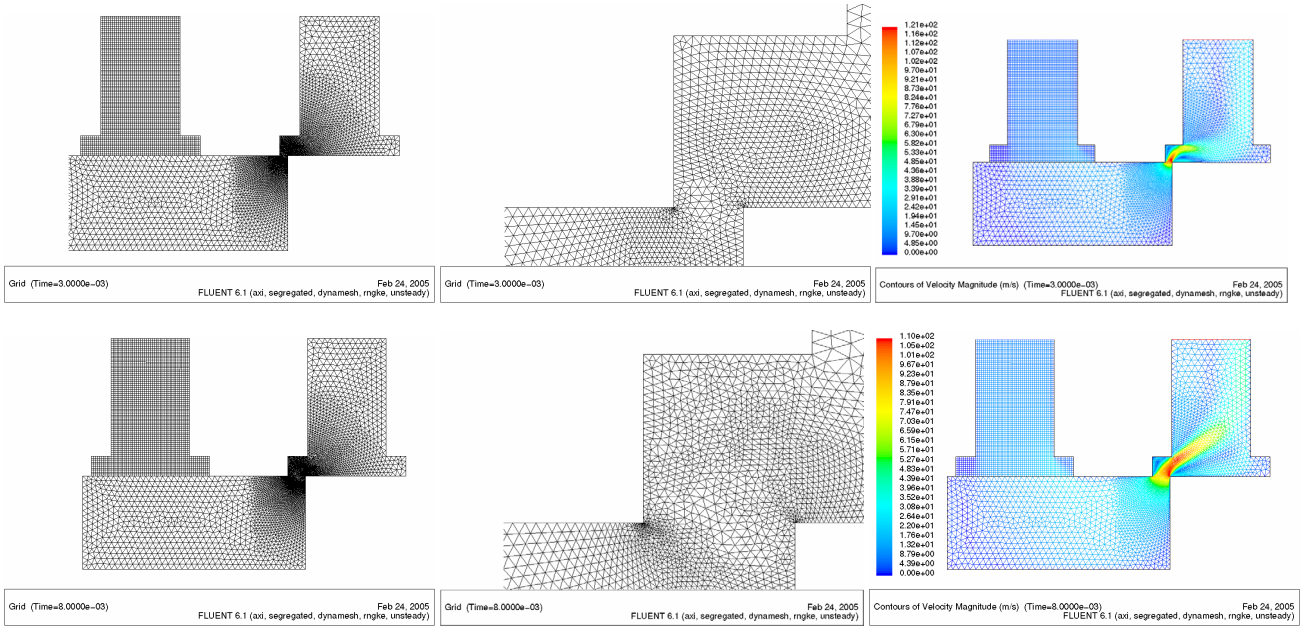

Fig. 3: *"Dynamic mesh" process during the spool movement and velocity contours (0.3 and 0.8 mm axial spool openings)*

As far as the flow forces are concerned, (Fig. 6 and Fig. 7) the values computed in the unsteady case are significantly greater if the spool opening time equals 2 ms while the difference is less evident if the opening time is 20 ms.

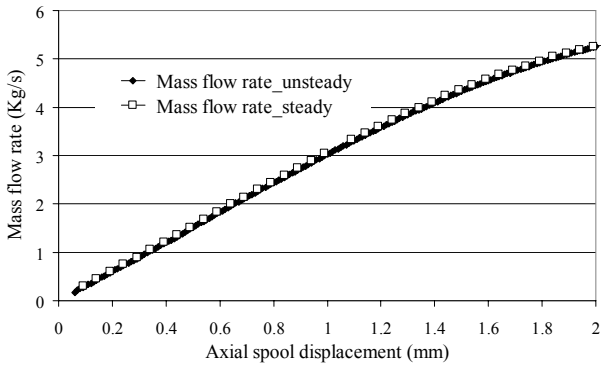

Fig. 4: *The discharged mass flow rate: unsteady vs steady (case 30 bar, 20 ms)*

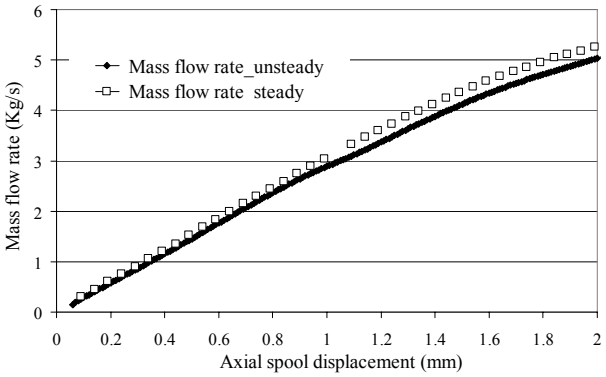

Fig. 5: *The discharged mass flow rate: unsteady vs steady (case 30 bar, 2 ms)*

In order to better analyze the differences between unsteady and steady results three different terms can be identified starting from Eq. 17.

The first term derives from the viscous effects:

$$\Delta F_{\_\text{visc}} = F_{\text{sleeve\_unsteady}} - F_{\text{sleeve\_steady}} \tag{18}$$

the second one derives from different efflux conditions in the inlet and metering sections (see Fig. 1):

$$\Delta F_{\_\text{efflux}} = (M_{2\text{ax}} - M_{1\text{ax}})_{\text{unsteady}} - (M_{2\text{ax}} - M_{1\text{ax}})_{\text{steady}} \tag{19}$$

the third term derives from the unsteady inertial term:

$$\Delta F_{\_\text{inertial}} = \rho L_1 \dot{Q} \tag{20}$$

The flow rate time derivative has been analytically estimated starting from the results presented in the diagrams of Fig. 4 and 5.

In addition to the three components, Fig. 8 and Fig. 9 show the term $\Delta F_{\_\text{global}}$ as the difference between the steady and unsteady global flow forces computed by Fluent™ i.e.:

$$\Delta F_{\_\text{global}} = F_{\text{unsteady}} - F_{\text{steady}} \tag{21}$$

These terms are derived from the numerical integration of the pressure and viscous forces on the surfaces of the spool.

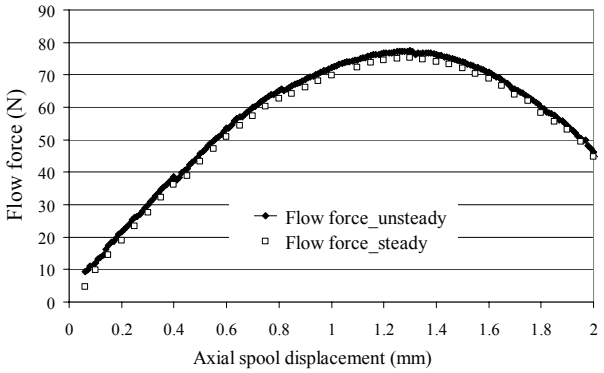

Fig. 6: *The flow force: unsteady vs steady (case, 30 bar, 20 ms)*

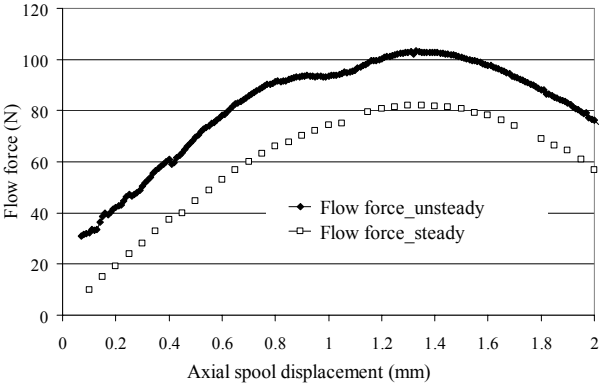

Fig. 7: *The flow force: unsteady vs steady (case, 30 bar, 2 ms)*

From the previous diagrams the following observations can be derived:

- the first component deriving from the unsteadiness of the viscous effects is negligible,
- the component that refers to the efflux conditions is appreciable only in the case of 2 ms spool opening time while in the other situation it is negligible,
- the third component is primarily responsible for the difference between steady and unsteady solution in both cases.

The global difference $\Delta F_{\_\text{global}}$ (that is the rigorous difference between steady and unsteady flow forces) is not exactly the algebraic sum of the three terms. This is due to the approximation concerning the length L_1 and to numerical inaccuracy problems.

In order to better analyze the efflux conditions in the steady and unsteady simulations, the traditional orifice equation connecting the flow rate to the pressure drop and the opening section can be considered:

$$Q(A_2,t) = C_\text{d}(A_2,t)A_2(t)\sqrt{\frac{2\Delta p}{\rho}} \tag{22}$$

According to the quasi-static assumption the value of the discharge coefficient C_d is dependent only on the opening section area. For this reason the value of the steady state discharge coefficient can be considered valid in unsteady conditions at the same opening area. This assumption enforces that the effects deriving from the unsteadiness of the fluid dynamic field on the efflux conditions are negligible.

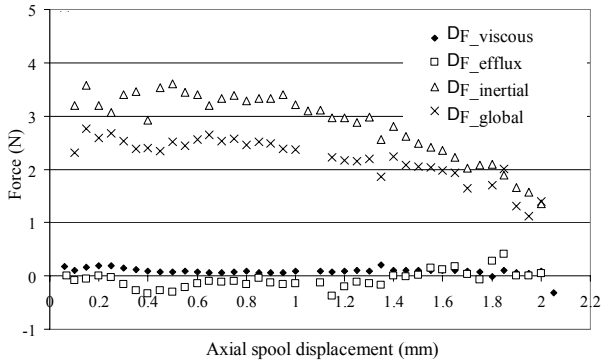

Fig. 8: *Unsteady corrections (case 30 bar, 20 ms)*

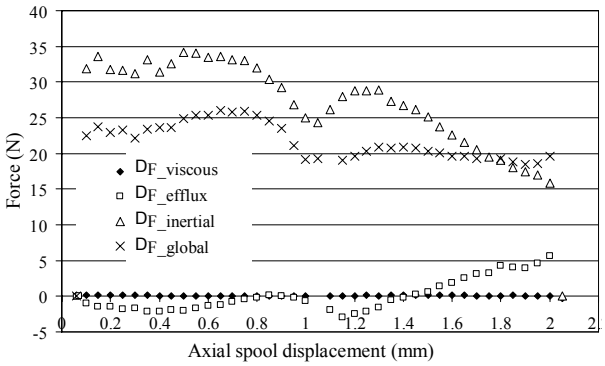

Fig. 9: *Unsteady corrections (case 30 bar, 2 ms)*

The last effects can be summarized as follows :

- the influence of the boundary layer,
- the average fluid dynamic angle,
- the average pressure value in the vena contracta,
- the ratio of vena contracta area to the the geometrical restricted area.

By using the numerical results provided by the code, it is possible to make a comparison between the efflux conditions in the unsteady and steady simulations in order to test directly the validity of the pseudo-steadiness hypothesis.

The diagram of Fig. 10 presents the ratio $v_{max}/\overline{v}$ of the maximum velocity value to the average value in the restricted section. This ratio can be considered representative of the boundary layer effects on the velocity profile in the metering section.

The diagram of Fig. 11 presents the ratio:

$$R = \frac{p_{outlet} - \overline{p}}{\Delta p} \tag{23}$$

where p_{outlet} is the enforced pressure outlet and $\overline{p}$ is the average pressure value in the restricted section.

This ratio indicates the level of pressure recovery in the zone between the restricted section and the outlet section.

In both diagrams only if the opening time equals 2 ms some differences can be appreciated.

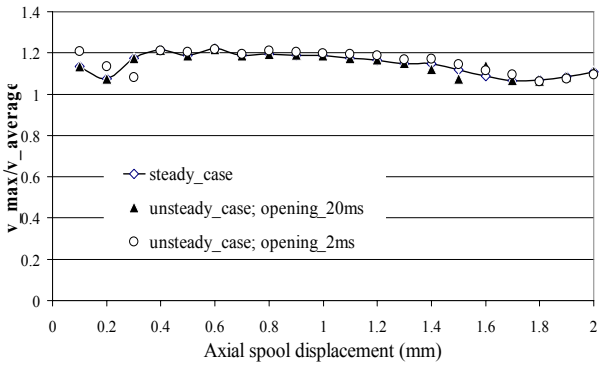

Fig. 10: *Boundary layer effects*

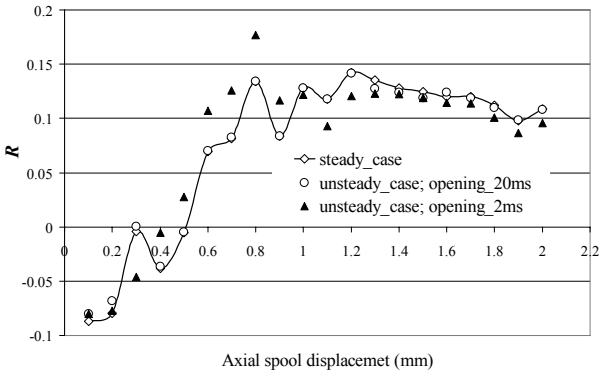

Fig. 11: *Pressure recovery effects*

The diagrams of Fig. 12 and 13 refer to the values of the average fluid dynamic angle υ_2 (see Fig. 1); only the case relative to the greater spool velocity shows an appreciable difference. In particular the angles computed in the case of faster spool movement are lower (i.e. more axial) than the angle values provided by the steady simulations. This behaviour can be easily physically explained: the axial flow in the channel tends to preserve, because of its inertia, the axial direction in spite of the radial deviation caused by the spool wall.

The last results show that, with a 20 ms spool opening time, the pseudo-steadiness hypothesis is perfectly confirmed while non-negligible differences in the efflux angle values arise when the spool velocity is greater.

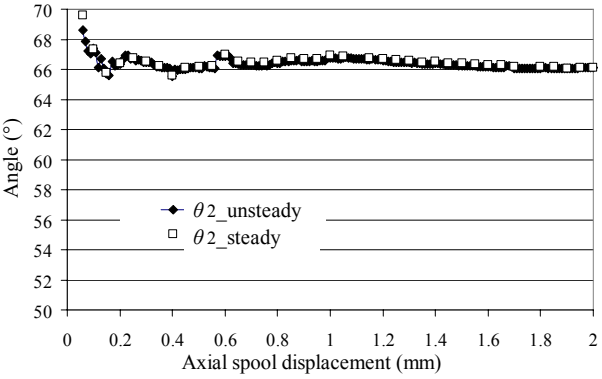

Fig. 12: *Average fluid dynamic angles (case 30 bar, 20 ms)*

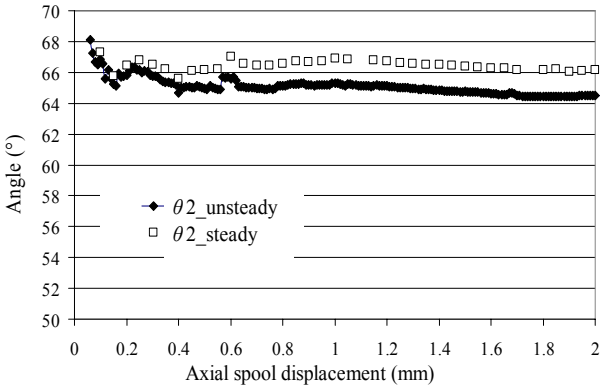

Fig. 13: *Average fluid dynamic angles (case 30 bar, 2 ms)*

In order to understand the influence of pressure drop, another simulation, with 80 bar pressure drop and 20 ms spool opening time, has been realized. The inertial term changes in the range 2.5 - 6 N while the peak value is 220 N (refer to Fig. 14 and 15); it can be noticed from the diagram of Fig. 8 that the inertial term in the case of 30 bar pressure drop is in the range 1.5 - 4 N while the peak flow force value equals approximately 75 N.

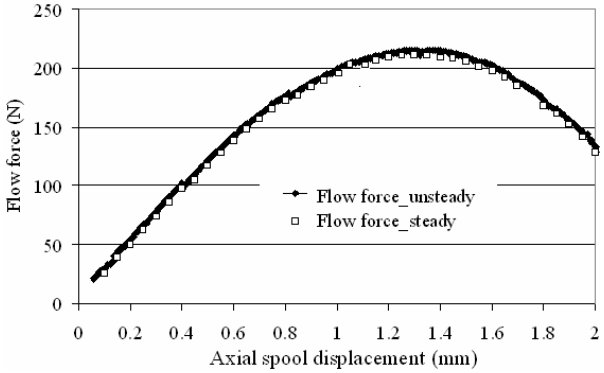

Fig.14: *flow force (case 80 bar, 20 ms)*

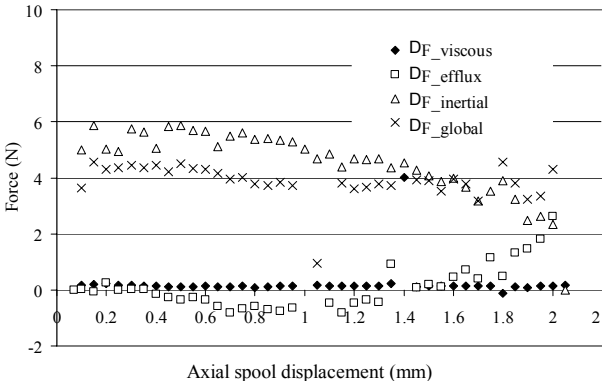

Fig.15: *Unsteady corrections (case 80 bar, 20 ms)*

The numerical results show that the percentage importance of the inertial term decays rapidly with the increasing pressure drop.

To better explain the last results the average axial velocity values in the INLET and OUTLET sections can be considered and the Eq. 17 can be expressed in the following alternative formulation:

$$F_{\text{spool}} = \rho Q\left(\overline{v_{2\text{ax}}} - \overline{v_{1\text{ax}}}\right) + \rho L\dot{Q} + F_{\text{sleeve}} \qquad (24)$$

or in a more explicit form:

$$F_{\text{spool}} = F_{\text{sleeve}} + \rho Q^2\left[\frac{1}{A_2 tg\,\overline{\vartheta_2}} - \frac{1}{A_1 tg\,\overline{\vartheta_1}}\right] + \rho L\dot{Q} \qquad (25)$$

Considering the orifice equation (Eq. 22) the flow force can be, finally, expressed as follows:

$$F_{\text{spool}} = F_{\text{sleeve}} + 2\Delta p\left[\frac{C_{\text{d}}^2(t)A_2}{tg\,\overline{\vartheta_2}} - \frac{C_{\text{d}}^2(t)A_2^2}{A_1 tg\,\overline{\vartheta_1}}\right] + \rho L\left[A_2\sqrt{\frac{2\Delta p}{\rho}}\frac{dC_{\text{d}}}{dt} + \frac{dA_2}{dt}C_{\text{d}}\sqrt{\frac{2\Delta p}{\rho}}\right] \qquad (26)$$

In the Eq. 26, it is evident that the inertial component is proportional to the square root of the pressure drop while the other terms, connected with the momentum flow values, are linearly proportional to the pressure drop.

For the last reason the percentage importance of the inertial term decreases with the increasing pressure drop enforced on the valve.

5 Pressure Ripple with a Fixed Spool Opening

In order to analyze the effects of the variable boundary conditions on the fluid dynamic behaviour of the valve, this section will present the preliminary results dealing with a pressure ripple enforced on a fixed axial opening metering section.

The generic pressure ripple has the following expression:

$$\Delta p = \Delta p_0 + p_{\text{A}}\sin(\omega t) \qquad (27)$$

Different cases have been realized at a fixed spool opening with different ripple frequencies.

The flow rates and the flow forces have been compared with the results obtained at the same instantaneous pressure drop but in steady conditions.

As far as the mass flow rate diagram is concerned (Fig. 16), an evident phase lag and an amplitude attenuation can be noticed when the pulsation reaches 1 kHz value.

It is obvious that above the last pulsation value the quasi-static assumption fails.

Any evident difference between unsteady and steady cases is clearly notable if the pulsation value is lower than 100 Hz.

The amplitude attenuation can be physically explained: the inertial forces, needed to accelerate the mass of the fluid upstream and downstream of the metering section, require additional pressure drops.

It is evident that if the global pressure drop on the computational domain is kept at a constant value, the last phenomenon reduces the pressure drop on the metering section so reducing the flow rate values crossing the valve.

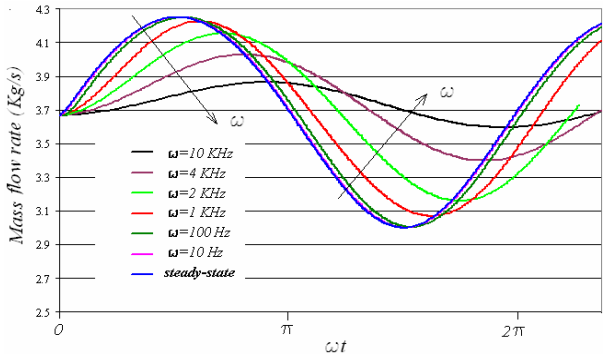

Fig. 16: *Mass flow rate profiles at different pressure ripple pulsations*

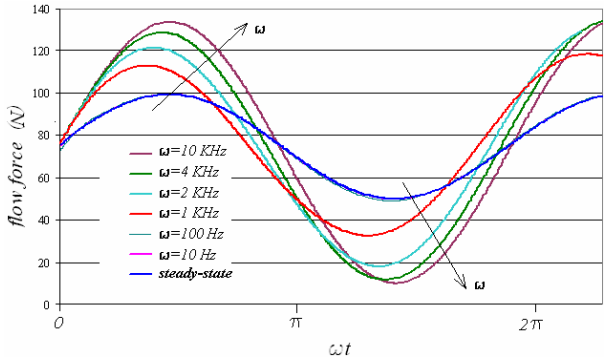

Fig. 17: *Flow force profiles at different pressure ripple pulsations*

With reference to the diagram of the Fig. 17, the global flow force values increase with the increasing pulsation value and this phenomenon is evident only when the pulsation value is greater than 1 kHz.

The unsteady flow force profiles are easily explained because the inertial components of the unsteady forces increase with the increasing acceleration of the fluid that is directly connected to the pressure ripple frequency.

6 Pressure Damped Oscillations During the Spool Travel

This section will show the fluid dynamic behaviour of the valve when the spool is subjected to a pressure inlet oscillation during its travel.

It must be considered that these oscillations can be derived from the dynamic response of the hydraulic circuit connected to the valve.

In particular a damped pressure oscillation has been enforced on the Inlet section during the spool travel using the expression of the dynamic response of a generic under damped 2nd order system i.e.:

$$\Delta p = \Delta p_0 + p_A \frac{e^{-\delta\omega_n t}}{\sqrt{1-\delta^2}} \sin\left(-\omega_n \sqrt{1-\delta^2}\, t\right) \qquad (28)$$

The natural pulsation and the damping factor have been computed enforcing a certain number of oscillations during the spool travel and a fixed value of the attenuation of the final amplitude (2%).

Table 1 illustrates the values of the natural pulsation and of the damping factors. The spool opening time is kept at a constant value of 12 ms.

The diagrams of Fig. 18, 19 and 20 will show the flow rate and the flow forces profiles in the following cases:

- 6 oscillations
- 30 oscillations
- 60 oscillations

compared with the steady state conditions.

Table 1: Damped pressure oscillations parameters

	6 oscillations	30 oscillations	60 oscillations
Natural pulsations (Hz)	500	2500	5000
Damping factor	0.1	0.02	0.01

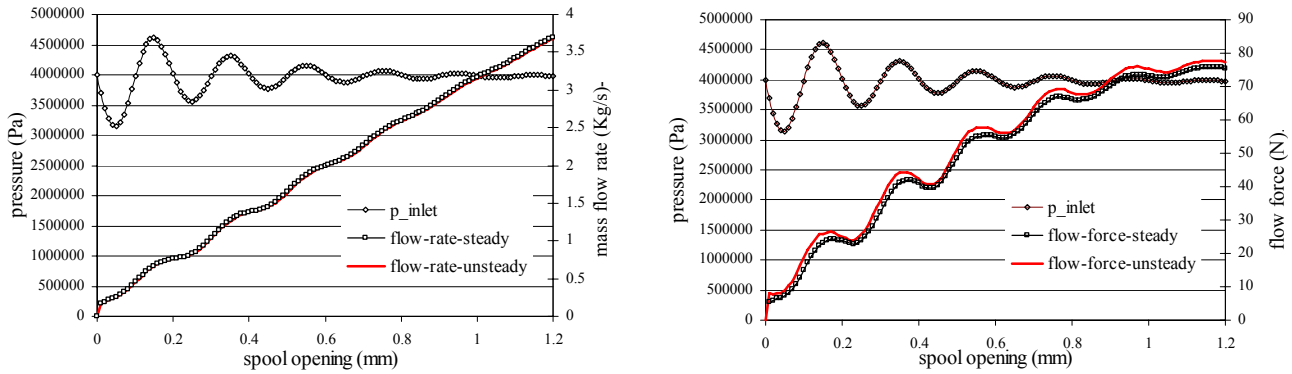

Fig. 18a: *6 damped oscillations during the spool opening (mass flow rate and flow force)*

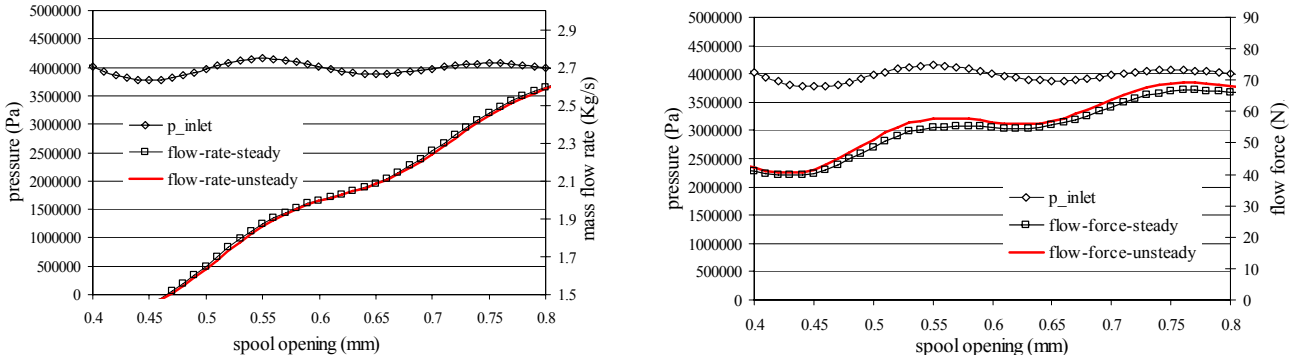

Fig. 18b: *6 damped oscillations, zoomed images (mass flow rate and flow force)*

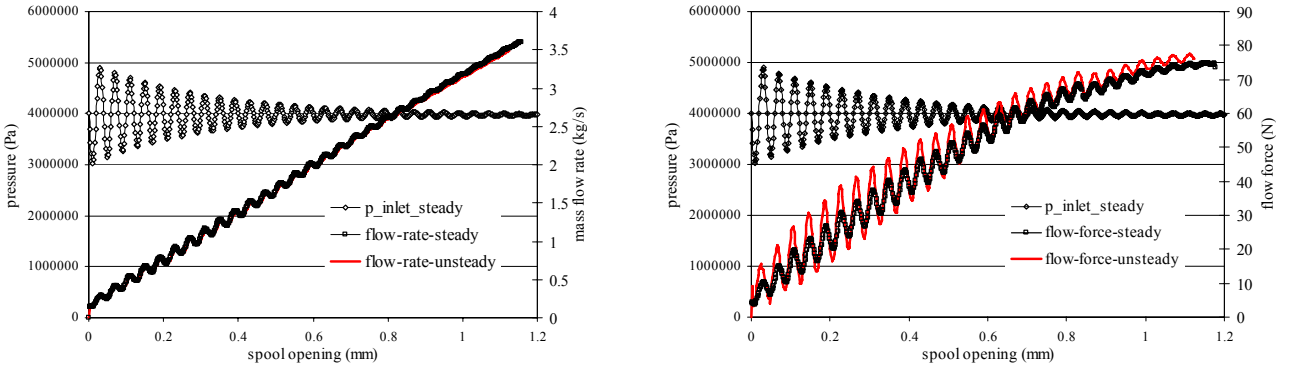

Fig. 19a: *30 damped oscillations during the spool opening (mass flow rate and flow force)*

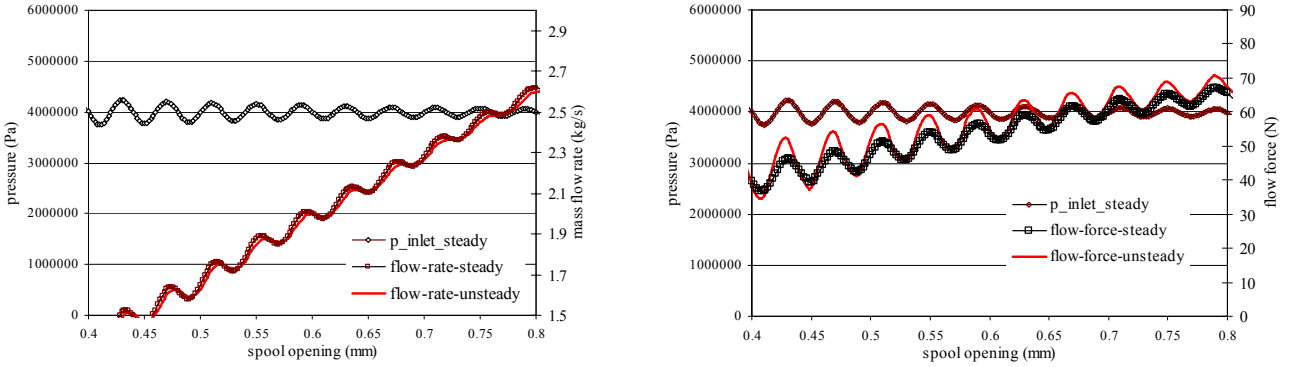

Fig. 19b: *30 damped oscillations, zoomed images (mass flow rate and flow force)*

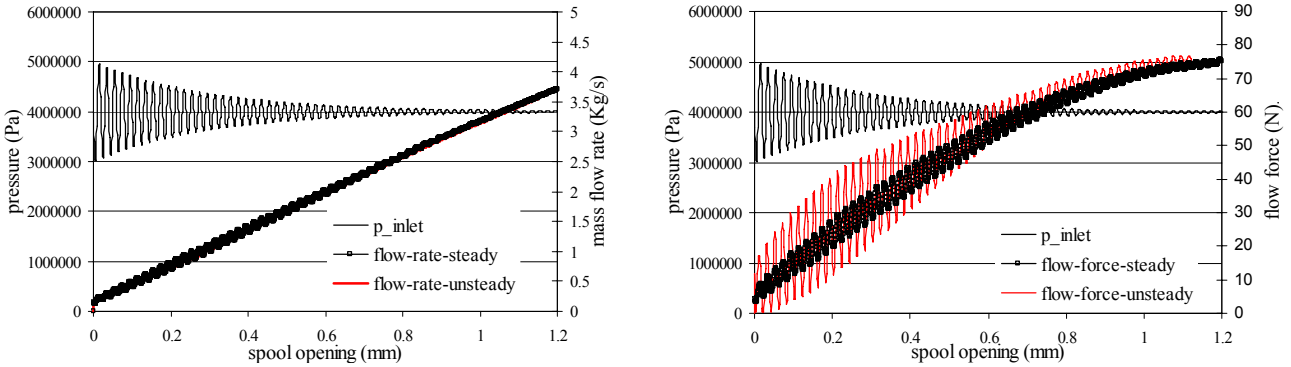

Fig. 20a: *60 damped oscillations during the spool opening (mass flow rate and flow force)*

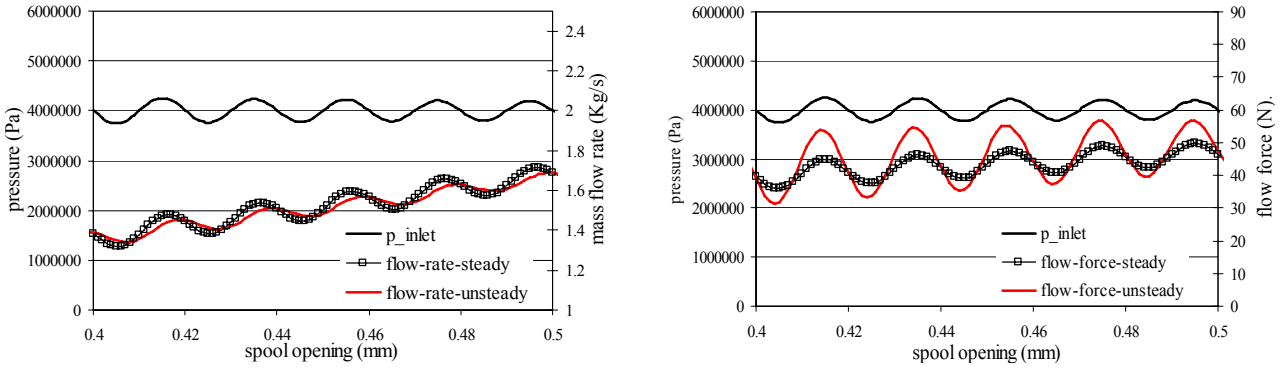

Fig. 20b: *60 damped oscillations, zoomed images (mass flow rate and flow force)*

The zoomed images show a phase lag and an amplitude attenuation of the flow rate increasing with the pulsation frequency. The flow force profiles show a notable amplitude amplification due to the inertial effects when the natural pulsation equals 5 kHz .

A general conclusion from the last two sections is that the pseudo-steadiness hypothesis fails if the pressure oscillation frequency reaches values around 1 kHz in the case of pressure ripple either at a fixed spool opening or during the axial spool opening.

In fact in these cases the flow rate computed in steady state conditions at the same pressure drop and spool opening values is not valid in the transient phases because a non-negligible phase lag and amplitude attenuation must be considered.

As far as the flow forces are concerned an additional term increasing with the pressure pulsation is always present and its percentage importance increases with the increasing pressure pulsation. It is obvious that in a design phase of the driving system such amplification of the flow forces must be considered if the hydraulic circuit dynamic response could produce pressure ripple pulsation above 1 kHz.

6 Conclusions

This paper shows, by means of a complete numerical unsteady analysis, the limitations of the efflux conditions pseudo-steadiness hypothesis for hydraulic spool valves used in fluid power applications.

The hypothesis can be considered absolutely valid in the case of typical spool velocity values (around 0.1 m/s) and for constant pressure boundary conditions. In the last conditions the steady numerical simulations can offer a good estimation of the flow rate and flow force trends during the spool opening.

The flow rate profile, computed by means of steady state investigations, can be considered valid in the unsteady state conditions because the fluid dynamic phenomena evolve with time scales that are always much lower than the spool movement ones.

As far as the flow forces are concerned, the inertial component must be added to the steady flow force value and can be analytically evaluated by assuming simplifying theoretical hypotheses.

This analysis has shown that the percentage importance of the inertial component decreases with the increasing pressure drop and can be neglected if the pressure drops reach the usual values of fluid power applications.

The last conclusions are valid in the case of commercial traditional valves. ON-OFF or proportional valves with higher dynamics (velocity around 1 m/s) certainly require a rigorous unsteady numerical analysis. In fact, the efflux conditions can change significantly in unsteady conditions and moreover the inertial term becomes important if compared to the global flow force value.

In particular, the inertial term has a remarkable importance if the pressure drop on the metering section decreases. Moreover, in the case of higher dynamics, the difference between steady and unsteady average efflux angles can produce a non-negligible error in the estimation of the flow rate profile during the axial spool opening.

When the pressure boundary conditions are not constant the pseudo-steadiness hypothesis can be considered valid if the pressure dynamics is characterized by frequency values below a magnitude order of 1 kHz. In fact, above this value, the flow rate profile presents a remarkable phase lag and an amplitude attenuation; moreover the inertial term of the flow force (proportional to the pressure pulsation value) could have a relevant percentage importance increasing the amplitude of the flow force ripple during the opening phase.

Nomenclature

A_r	metering section area
a_{spool}	spool acceleration
CV	control volume
C_d	discharge coefficient
D	spool external diameter
d	spool internal diameter
$\bar{f}$	body forces per unit mass
F_{sleeve}	force acting on the sleeve
F_{spool}	flow force on spool
L	length of the control volume
L_1	damping length
Q	flow rate
$\bar{p}$	average pressure value in the metering section
p_A	amplitude of pressure ripple

p_{inlet}	enforced inlet total pressure
p_{outlet}	enforced outlet static pressure
r	radial distance from spool axis
v_r	normal velocity in the restricted section
v_{spool}	spool velocity
w	pulsation of pressure ripple
x	spool axial travel
$\bar{v}$	average velocity value in the metering section
β	bulk modulus
δ	damping factor
Δp	pressure drop
Δp_0	average value of pressure ripple
$\bar{\sigma}$	stress vector
Πc	unsteady terms ratio
Πi	unsteady terms ratio
Πv	unsteady terms ratio
ρ	fluid density
ω_n	natural pulsation

References

Batoli, M. 1996. Analisi teorico-sperimentale delle forze di flusso in un distributore a comando elettrico, *Oleodinamica e Pneumatica*.

Borghi, M., **Milani, M.** and **Paoluzzi, R.** 2000. Stationary axial flow force analysis on compensated spool valves, *International Journal of Fluid Power* 1 No. 1 p.p. 17-25.

Borghi, M., **Milani, M.** and **Paoluzzi, R.** 1998. Transient flow force estimation on the pilot stage of a hidraulic valve; *Proceedings of the ASME-IMECE FPST, Fluid Power SYSTEMS & Tech,* Vol.5 pp. 157-162.

Del Vescovo, G. and **Lippolis, A.** 2002. Flow forces analysis on a four way valve, *Proceedings of 2nd FPN PhD International Symposium*, Modena, Italy.

Del Vescovo, G. and **Lippolis, A.** 2003. Three-dimensional analysis of flow forces on directional control valves, *International Journal of Fluid Power*, Vol. 4 Number 2.

Del Vescovo, G. and **Lippolis, A.** 2003. CFD analysis of flow forces on spool valves, *Proceedings of the 1st International Conference on Computational Methods in Fluid Power Technology*, Melbourne November 26-28.

Fluent Inc. 1995. *Fluent Europe user's guide.* Vol. 1-4 .

Fluent Inc. 1995. *Fluent tutorial guide* Vol.1,2 .

Fluent Inc. 2000. *Gambit user's guide.*

Fluent Inc. 2000. *Gambit Modeling guide.*

Huguet, D. 2004. Dynamic mesh of a direct acting relief valve, *Proceedings of the 3rd Fluid Power Net International PhD Symposium*, Terrassa, Spain.

Krishnaswamy, K. and **Li, P.Y.** *2002.* On Using Unstable Electrohydraulic valves for control; *Journal of dynamic systems, Measurement and control,* March 2002 Vol. 124.

Macor, A. 2002. Analisi sperimentale di un distributore oleodinamico con sezione ristretta a intaglio piano. *Proccedings of 57° Congresso Nazionale ATI*, Pisa.

Macor, A. and **Badin, D.** 1999. Influenza dei modelli di turbolenza nello studio delle forze di flusso nei distributori oleoidraulici, *Proceedings of 54° Congresso Nazionale ATI*, L'Aquila.

Macor, A. and **Dato, S.** 2000. La riduzione delle forze di flusso in un distributore oleoidraulico mediante sagomatura della sezione ristretta, *Proceedings of 55° Congresso nazionale ATI*, Bari-Matera.

Merrit, H. E. 1967. *Hydraulic Control Systems*, John Wiley & sons.

Nervegna, N. 2000. *Oleodinamica e Pneumatica*, Sistemi - Vol.1., Torino: Politeko.

Yang, R. 2006. Hydraulic oil flow wall shear effect on valve actuator flow forces, *Proceedings of the 2nd International Conference on Computational Methods in Fluid Power Technology*, Aalborg, Denmark.

Giuseppe Del Vescovo
Born in Bari (BA) in 1975. Graduated in Mechanical Engineering (2000) at the Politecnico di Bari, Italy. In April 2005, he received his PhD in Mechanical Engineering from the Politecnico di Bari. Author and Co-Author of 15 papers dealing with the application of CFD and experimental techniques in the analysis of flows in hydraulic and pneumatic valves.

Antonio Lippolis
Born in Gioia del Colle (BA) in 1955. Graduated in Mechanical Engineering (1981) at the Politecnico di Bari (Italy). Researcher at the Faculty of Engineering of the Politecnico di Bari since 1983, at present is Professor in Fluid Power Systems. Author and Co-Author of more than 40 papers dealing with "Numerical Fluid-Dynamics" and "Fluid Power".